PHYSICAL REVIEW B **77**, 035212 (2008)

Fluorescence-detected magnetic resonance in organic systems: A pair-density matrix formalism approach

L. Hachani,[1] A. Benfredj,[1] S. Romdhane,[1,2] M. Mejatty,[1] J. L. Monge,[3] and H. Bouchriha[1]
[1]*Unité Matériaux Avancés et Optronique, Faculté des Sciences de Tunis, Campus Universitaire, 1008 Tunis, Tunisia*
[2]*Faculté des Sciences de Bizerte, Zarzouna, 7021 Bizerte, Tunisia*
[3]*Institut des Nano Sciences de Paris, 140 Rue de Lourmel, 75015 Paris, France*

(Received 9 March 2006; revised manuscript received 18 October 2007; published 29 January 2008)

A theoretical approach, based on a pair-density matrix formalism, is developed for the study of the dynamic triplet-pair annihilation in organic materials. Stochastic Liouville equation, taking into account effects of static and dynamic magnetic fields, with superoperators representing coherent evolution, spin-independent annihilation rate, spin-dependent recombination, and diffusion of triplet exciton pairs, is used. This approach is applied to analyze fluorescence detected magnetic resonance (FDMR) spectra of one-dimensional and two-dimensional exciton motion systems. The nearest-neighbor and the long-range mutual annihilations of triplets are taken in account, and the S_0Q_0 mixing, in triplet-pair states, is pointed out. The long-range annihilation rate λ and the triplet effective decay rate β are determined from the best fit with experimental FDMR spectra.

DOI: 10.1103/PhysRevB.77.035212 PACS number(s): 32.50.+d, 71.35.−y

I. INTRODUCTION

Modulation by static magnetic field of delayed fluorescence (DF) due to triplet-triplet exciton annihilation in molecular crystals and other π-conjugated systems has been studied since the 1970s and continues to attract great attention recently up to now.[1–18] In these crystals, triplet excitation migration may proceed from molecule to another on a time scale, which is short compared with the long triplet state lifetime but which is long compared with the normal fluorescence lifetime. Nearest-neighbor and long-range mutual interactions of two triplets may then take place. Free triplets come together and form a correlated state (T,T), which can undergo fusion via the singlet channel or the triplet one (fusion via quintet channel is energetically unfavorable). The process, in which the excited state S^* is populated by the (T,T) pair annihilation, produces one molecule in the S^* state whose lifetime is much longer than the spontaneous fluorescence, hence the name of delayed fluorescence. The following scheme is used to interpret this phenomenon:

$$T+T\rightarrow(T,T)\rightarrow S^*\rightarrow S_0+\underbrace{h\nu}_{DF},$$

where T stands for free-triplet exciton, (T,T) for bound pair, S^* for the excited singlet exciton, S_0 for the ground singlet state, and $h\nu$ corresponds to the delayed fluorescence.

The kinetic equations for this fusion process are

$$dn/dt = I-\beta_n n-\gamma n^2, \qquad (1)$$

$$dp/dt = \gamma n^2/2-\beta_p p-\alpha_p p, \qquad (2)$$

with I uniform creation of free excitons, n and p the densities of free excitons and bound pairs, β_n and β_p are the inverse lifetimes of free excitons and bound pairs, γ quadratic interaction of free excitons, and α_p annihilation of bound pairs giving an excited singlet state. In steady-state conditions and in low illumination excitation ($\beta_n n \gg \gamma n^2$), these equations rise to

$$Fluorescence \approx \alpha_p p = \alpha_p\gamma n^2/(\alpha_p+\beta_p)/2. \qquad (3)$$

This equation shows the quadratic dependence of the fluorescence on the density of created free excitons, but it needs an elaborate theory for γ computation to take the magnetic field effects into account. These macroscopic equations suggest a stochastic Liouville equation (SLE) with the bound pairs density matrix ρ (instead of p) as a solution. The SLE is defined in a nine-dimensional Hilbert space with a Hamiltonian depending only on spin operators. The nine eigenfunctions of spin operators $\mathbf{S}^2$ and S_z are quintuplet $Q(S=2,m_s=0,\pm1,\pm2)$, triplet $T(S=1,m_s=0,\pm1)$, and singlet $S(S=0,m_s=0)$; $\mathbf{S}^2$ is the square of the total spin of the exciton triplets pair [$\mathbf{S}=\mathbf{s}(1)+\mathbf{s}(2)$, $\mathbf{s}(1)$, and $\mathbf{s}(2)$ are the spins of each exciton] and S_z its z component.

The pair density matrix which, for a uniform system, depends on the relative position $\mathbf{r}$ of two excitons is denoted by $\rho(\mathbf{r},t)$ and satisfies the following SLE:

$$\frac{\partial\rho(\mathbf{r},t)}{\partial t} = \underbrace{-\frac{i}{\hbar}[\mathcal{H}_p,\rho(\mathbf{r},t)]}_{Liouville\ term}\underbrace{-2\beta_n\rho(\mathbf{r},t)}_{decay\ term}\underbrace{-\frac{1}{2}\lambda(r)[\tilde{\Lambda},\rho(\mathbf{r},t)]^+}_{annihilation\ term} \underbrace{+2\mathcal{D}\nabla^2\rho(\mathbf{r},t)}_{diffusion\ term}\underbrace{+Q(\mathbf{r},t)}_{source\ term}+\underbrace{\left(\frac{\partial\rho(\mathbf{r},t)}{\partial t}\right)_{rel}}_{spin\ relaxation\ term}, \qquad (4)$$

where $[\ldots,\ldots]$ stands for commutator and $[\ldots,\ldots]^+$ for anticommutator, $\mathcal{H}_p$ is the spin Hamiltonian of the bound pair, $\tilde{\Lambda}=sP_S+tP_T+qP_Q$, where P_S, P_T, and P_Q are, respectively, projection operators onto the singlet, the triplet, and the quintet manifolds of the pair states, the scalars s, t, and q are the corresponding weights at high static magnetic field ($s=0.66$, $t=0.33$, and $q=0.01$), $\mathcal{D}$ the diffusion tensor of each element of the pair, and finally, $Q(\mathbf{r},t)=I_H/9$, where I_H is the matrix identity in Hilbert space.

1098-0121/2008/77(3)/035212(7)

We could rewrite Eq. (4) in the compact form,

$$\frac{\partial\rho(\mathbf{r},t)}{\partial t}=[-\mathcal{C}(\mathcal{H}_p)-2\beta_n I_L-\lambda(r)\mathcal{A}(\tilde{\Lambda})+\mathcal{R}+2D\nabla^2]\rho(\mathbf{r},t)+Q(\mathbf{r},t). \qquad (5)$$

Here, $\mathcal{C}$ is the superoperator commutator which is multiplied by $2\pi i$. Moreover, $\mathcal{A}$ is the superoperator anticommutator divided by 2, I_L denotes the identity supermatrix in Liouville space, and $\mathcal{R}$ is the Redfield supermatrix of spin relaxation in frequency units. $\mathcal{H}_p$ is expressed in frequency units, while $\tilde{\Lambda}$ is dimensionless.

Giving that spin angular momentum is conserved between pair states and the excited singlet state, the observable (fluorescence) should be proportional to $(\beta_n \int_{sample}\lambda(r)\mathrm{Tr}[P_S\rho(\mathbf{r},t)]dv)$.

Johnson and Merrifield (JM)[19] were the first to use a SLE with the following simplifications: **r** is a constant with an undetermined value, therefore, there is no **r** dependence and there is neither spin relaxation nor diffusion. The spin Hamiltonian is just the sum of Hamiltonians of each exciton forming the pair with no interaction. So JM have interpreted the magnetic field effects (MFEs) on DF in anthracene crystals. The theory did not give perfect fits with experimental results, but it paved the way to improve the understanding of these problems. The published values of $(2\beta_n)$, noted k_{-1} in Ref. 19, are around $2.5\times10^9\ \mathrm{s}^{-1}$ for anthracene.

Suna elaborated a kinematic approach,[20] which explicitly takes into account the dimensionality of the free-triplet hopping transport. The parameters of the kinematic theory are then the nearest-neighbor pair transition rate toward the singlet manifold λ, and the effective, for the correlated-pair formation, decay rate $\beta_{effective}$ of the unpaired exciton which, in one and two dimensions, is determined by the out-of-main-dimension hopping rate Ψ_{out} eventually perturbed by the rate of triplet spin relaxation. The correlated-pair lifetime $(2\beta_n)^{-1}$ should be sufficiently long compared with the exciton residence time on a site $1/\Psi$, Ψ being the total hopping rate out from the site in the main dimension of motion so that repeated collisions and pair reformation become possible.[23]

In the anthracene case where the motion is anisotropic with two dimension in the monoclinic *ab* plane with the main value of the diffusion tensor such that $D_{aa}=D_{bb}$ and $D_{cc}\approx0.1D_{aa}$,[21,22] and two excitons being in two different *ab* planes having no chance to reencounter, the hopping rate out of the *ab* planes $\Psi_c^*=D_{c^*c^*}/(c^*)^2$, where c^* is the distance between *ab* planes ($\mathbf{c}^*$ is a vector parallel to $\mathbf{a}\times\mathbf{b}$). The intrinsic exciton decay rate $\beta_n^0\approx10^3\ \mathrm{s}^{-1}$ is negligible compared to Ψ_c^*, which therefore is just the effective decay rate. Thus, $\beta_{effective}=\beta_n=\Psi_c^*$ (by analogy with previous papers, we will note β instead of β_n).

To overcome the diffusion problem, Suna introduced the boundary $r=R$ and took for the nearest-neighbor interaction function the definition

$$\lambda(r)=\lambda,\quad R_0<r<R,$$

$$\lambda(r)=0,\quad r>R,$$

and the continuity of the stream of excitons at $r=R$. The excluded volume $r<R_0$ represents the impossibility of two excitons to occupy the same lattice site.

Using this theory to explain the magnetic field effect on DF, we found for anthracene crystals (unpublished results) $\beta=2.2\times10^9\ \mathrm{s}^{-1}$ and $\lambda=5\times10^{11}\ \mathrm{s}^{-1}$. However, several other fits can be obtained with other parameters and even with $\lambda=5\times10^{13}\ \mathrm{s}^{-1}$ or using one-dimensional (1D) or three-dimensional (3D) triplet exciton motion functions. Moreover, we did not have a good agreement between the result obtained within this theory and the experimental data for the magnetic field effect on DF in the case of crystals, where the rate of triplet spin relaxation is important such as 1,4 dibromonaphtalene (1,4 DBN), naphtalene, paraterphenyle, and pyrene. In fact, the calculation of γ becomes considerably more complex when spin relaxation is included, since relaxation causes incoherent transitions among the various spin states which are stationary with respect to the spin Hamiltonian $\mathcal{H}_p$. The equation of motion for the pair density matrix can then no longer be separated. Furthermore, the separation between odd and even spin states cannot be achieved in general. Suna has proposed to use approximate expressions for spin relaxation effects on the annihilation rate, which are obtained with the following form for the spin relaxation of the two-exciton density matrix,

$$\left(\frac{\partial}{\partial t}\right)_{rel}\left[\rho(\mathbf{r})-\frac{1}{9}\mathrm{Tr}\,\rho(\mathbf{r})I\right]=-2\zeta\left[\rho(\mathbf{r})-\frac{1}{9}\mathrm{Tr}\,\rho(\mathbf{r})I\right]. \qquad (6)$$

According to Eq. (6), $\rho(\mathbf{r})$ is assumed to relax toward its local equilibrium value, a matrix corresponding to equal occupation of all pair spin states. The relaxation rate is the same for all matrix elements and is twice the average spin relaxation rate ζ because we are dealing with the relaxation of the spin of two excitons.

In a continuum model, $\lambda(r)$ is considered as a continuous decreasing function $[\lambda(r=\infty)=0]$. To have a model mathematically tractable and to represent as well as possible the physical reality, a partition on r space has been done as follows:

$$\begin{aligned}
&\lambda(r)=\lambda_\infty=\infty, && 0<r<r_a && \text{(nearest-neighbor interaction zone)},\\
&\lambda(r)=\lambda, && r_a<r<r_1 && \text{(long-range mutual interaction zone)},\\
&\lambda(r)=0, && r_1<r<\infty && \text{(noninteraction zone)},
\end{aligned}$$

where λ is the interaction constant, r_a and r_1 are, respectively, action and interaction radii. We consider $r=\infty$ when r is great with respect to the lattice parameters, the diffusion length, and the interaction length but small with respect to the macroscopic size of the samples. The mathematic resolution of the SLE implies the continuity of $\rho(r)$ and its derivative (continuity of the stream) at $r=r_a$ and $r=r_1$ with the boundary conditions $\rho(\infty)=n^2$ and $\rho(r\leqslant r_a)=0$; the last one represents the impossibility of two excitons to occupy the same lattice site (Ref. 11). By including triplet spin relaxation due to the modulation of local field by random jumps between nonequivalent sites in the crystal, for 1D (1,4 DBN),[23] two-dimensional (2D) (anthracene, naphtalene, and paraterphenyle),[11] and 3D (pyrene)[11] exciton motion systems, we have obtained good fits with the experimental results.

To our knowledge Mejatty *et al.* were the first to publish the fluorescence detected magnetic resonance (FDMR) spectra of anthracene crystals at room temperature.[24] They have noticed that when they include microwave effect in JM or Suna scheme,[24,25] they can reproduce qualitatively the FDMR spectra only by using, for the pair dissociation rate, values which were one order of magnitude smaller than the previously obtained ones for the MFE; i.e., $\beta=2.5\times10^8$ s^{-1}, (denoted k_{-1} in JM scheme,[23] $k_{-1}=6\times10^8$ s^{-1}).

Frankevich *et al.*[26] were the first authors to discover the delayed fluorescence intensity variations induced by microwave absorption on the fission of singlet excitons in tetracene. With JM's scheme one obtains $k_{-1}=2.2\times10^9$ s^{-1}, while the width of FDMR lines gives $k_{-1}=1.2\times10^8$ s^{-1}.[27]

Therefore, in both fusion of triplet excitons and fission of singlet excitons, as they are observed in (2D) exciton motion systems, respectively, anthracene and tetracene, some Liouville equations which are very convenient for MFE on DF are insufficient to explain the linewidth of FDMR spectra. The question is whether such problem can raised in (1D) exciton motion systems.

Recently, FDMR spectrum of a (1D) motion system, the 1,4 DBN, was reproduced using Suna's like theory.[28] Values were about 10^8 s^{-1} for β and 10^{10} s^{-1} for λ. However, we don't have values, for the static magnetic field effects, to do a comparison.

In the present work, we have adapted a previously published approach,[11] for static magnetic field effect on DF, to study the fluorescence detected magnetic resonances in 1D and 2D molecular crystals. We have included microwave effect to fit the FDMR spectra of 1,4 DBN and anthracene crystals.

II. THEORETICAL APPROACH

The magnetic field orientation effect on the fluorescence which is due to the interaction of two triplet excitons in organic crystals is an illustration of the S_0Q_0 mixing in the nine spin states of a triplets pair. While there is a large literature about S_0T_0 mixing in radicals recombination,[29] S_0Q_0 mixing in recombination of triplet excitons is rather ignored. However, the deep-set reason of this mixing is the same; the basis of spin functions in which the spin operators $\mathbf{S}^2$ and S_z are diagonal is not the eigenbasis of the spin Hamiltonian of the triplets pair $\mathcal{H}_p$.

TABLE I. Triplet-pair states energy levels.

Pair states	Energies
$\lvert 1\rangle=\frac{1}{\sqrt{3}}\lvert S_0\rangle+\sqrt{\frac{2}{3}}\lvert Q_0\rangle=\lvert T_0T_0\rangle$	$2\varepsilon_0$
$\lvert 2\rangle=\sqrt{\frac{2}{3}}\lvert S_0\rangle-\frac{1}{\sqrt{3}}\lvert Q_0\rangle=\frac{1}{\sqrt{2}}[\lvert T_{+1}T_{-1}\rangle+\lvert T_{-1}T_{+1}\rangle]$	$-\varepsilon_0$
$\lvert 3\rangle=\lvert Q_{+2}\rangle=\lvert T_{+1}T_{+1}\rangle$	$-\varepsilon_0+2g\mu_BH$
$\lvert 4\rangle=\lvert Q_{+1}\rangle=\frac{1}{\sqrt{2}}[\lvert T_{+1}T_0\rangle+\lvert T_0T_{+1}\rangle]$	$\frac{\varepsilon_0}{2}+g\mu_BH$
$\lvert 5\rangle=\lvert Q_{-1}\rangle=\frac{1}{\sqrt{2}}[\lvert T_{-1}T_0\rangle+\lvert T_0T_{-1}\rangle]$	$\frac{\varepsilon_0}{2}-g\mu_BH$
$\lvert 6\rangle=\lvert Q_{-2}\rangle=\lvert T_{-1}T_{-1}\rangle$	$-\varepsilon_0-2g\mu_BH$
$\lvert 7\rangle=\lvert T_{+1}\rangle=\frac{1}{\sqrt{2}}[\lvert T_{+1}T_0\rangle-\lvert T_0T_{+1}\rangle]$	$\frac{\varepsilon_0}{2}+g\mu_BH$
$\lvert 8\rangle=\lvert T_0\rangle=\frac{1}{\sqrt{2}}[\lvert T_{+1}T_{-1}\rangle-\lvert T_{-1}T_{+1}\rangle]$	$-\varepsilon_0$
$\lvert 9\rangle=\lvert T_{-1}\rangle=\frac{1}{\sqrt{2}}[\lvert T_{-1}T_0\rangle-\lvert T_0T_{-1}\rangle]$	$\frac{\varepsilon_0}{2}-g\mu_BH$

The Hamiltonian $\mathcal{H}_p(t)=\mathcal{H}_0+\mathcal{H}_{mw}(t)$ in which $\mathcal{H}_0$ is the sum of zero field splitting (ZFS) and Zeeman Hamiltonians of the two identical triplets without interaction: $\mathcal{H}_0=2\left[D^*(s_Z^2-\frac{1}{3}\mathbf{s}^2)+E^*(s_X^2-s_Y^2)+g\mu_B\mathbf{H}\cdot\mathbf{s}\right]$, where $\mathbf{s}$ is the spin of the triplet exciton, s_X, s_Y and s_Z are its components, D^* and E^* are the ZFS exciton parameters, and $\mathcal{H}_{mw}(t)$ the microwave perturbation Hamiltonian given by

$$\mathcal{H}_{mw}(t)=\frac{1}{2}g\mu_BH_1(S_+e^{-i\omega t}+S_-e^{+i\omega t}), \tag{7}$$

where H_1 is the amplitude of the microwave field, ω its frequency, and $S_\pm$ are spin operators. Eigenvectors and eigenvalues of the unperturbed Hamiltonian $\mathcal{H}_0$, at high static magnetic field, are given in Table I, where ε_0 is the energy of the $m_s=0$ level for the triplet exciton: $\varepsilon_0=D^*(\frac{1}{3}-n^2)+E^*(m^2-l^2)$. Here, l, m, and n are the cosine directors of the static field direction $\mathbf{H}$ with respect to the principal ZFS exciton axes. It should be noted that there is a S_0Q_0 mixing in $\lvert 1\rangle$ and $\lvert 2\rangle$ states.

The S_0Q_0 mixing is the main mechanism to understand the magnetic field effect on the delayed fluorescence; the other ones (diffusion and spin relaxation) must be considered to understand the mechanism of triplet-pair formation. Our aim is to give a good mathematical treatment of the diffusion to have a model as perfect as possible in order to verify all the hypothesis with experimental FDMR results.

After normalization of ρ by n^2 and in view to calculate in dimensionless units with respect to 2β, Eq. (5) can be rewritten, by neglecting triplet spin relaxation, in the following form:

$$\frac{\partial\rho(\mathbf{r},t)}{\partial t}=[-\mathcal{C}(\mathcal{H}_p)-I_L-\lambda(r)\mathcal{A}(\tilde{\Lambda})+r_d^2\nabla^2]\rho(\mathbf{r},t)+Q(r,t), \tag{8}$$

where $\mathcal{H}_p(t)=\mathcal{H}_p(t)/2\beta$, $\rho(\mathbf{r},t)=\rho(\mathbf{r},t)/n^2$, $\lambda(r)=\lambda(r)/2\beta$, and $r_d=\sqrt{2D/2\beta}$ where D is the one-, two-, or three-dimensional diffusion constant. Here, $\rho(\mathbf{r},t)$ is taken to have the form

$$\rho(\mathbf{r},t) = \rho^0(\mathbf{r}) + \tilde{\rho}(\mathbf{r})e^{i\omega t}, \tag{9}$$

Eq. (8) can be written as

$$\frac{\partial \mathbf{X}(\mathbf{r},t)}{\partial t} = -[\mathbf{A}(t) + \lambda(r)\mathbf{B} - r_d^2\nabla^2]\mathbf{X}(\mathbf{r},t) + \mathbf{Q_0}, \tag{10}$$

with

$$\mathbf{A}(t) = \mathrm{mat}\{\mathcal{C}[\mathcal{H}_0 + \mathcal{H}_{mw}(t) + \mathbf{I}_L]\},$$

$$\mathbf{X}(r,t) = \mathrm{col}[\rho(r,t)],$$

$$\mathbf{Q_0} = \mathrm{col}(I_H/9),$$

$$\mathbf{B} = \mathrm{mat}[s\mathcal{A}(P_S) + t\mathcal{A}(P_T) + q\mathcal{A}(P_Q)], \tag{11}$$

where mat$(\cdots)$ stands for matrix representation of a superoperator and col$(\cdots)$ stands for column representation of an operator (in a spin function basis); the numbering of column elements is done as usual.

Denoting

$$\mathrm{mat}[\mathcal{C}(\mathcal{H}_0 + \mathbf{I}_L)] = \mathbf{A_0},$$

$$\mathrm{mat}[\mathcal{H}_{mw}(t)] = \mathbf{A}_+e^{-i\omega t} + \mathbf{A}_-e^{+i\omega t},$$

$$\mathrm{col}[\rho(r,t)] = \mathbf{X}(r,t) = \mathbf{X_0}(r) + \tilde{\mathbf{X}}(r)e^{+i\omega t},$$

$$\mathbf{0} = \text{the zero column vector of size } 81, \tag{12}$$

Eq. (10) can be solved as

$$\begin{vmatrix} \mathbf{A_0} + \lambda(r)\mathbf{B} - r_d^2\nabla^2 & \mathbf{A}_+ \\ \mathbf{A}_- & \mathbf{A_0} + i\omega\mathbf{I}_L + \lambda(r)\mathbf{B} - r_d^2\nabla^2 \end{vmatrix} \cdot \begin{vmatrix} \mathbf{X_0}(r) \\ \tilde{\mathbf{X}}(r) \end{vmatrix} = \begin{vmatrix} \mathbf{Q_0} \\ \mathbf{0} \end{vmatrix}. \tag{13}$$

Given that the dimension of this system [Eq. (13)] is enormous 162 × 162, we just take into account only the diagonal elements and the off diagonal elements which connect levels with allowed transitions in the high-field approximation.

Since only six microwave induced transitions ($\Delta m_s = \pm 1$) are possible,[28] we reduce then $\mathbf{X}(r) = \begin{vmatrix} \mathbf{X_0} \\ \tilde{\mathbf{X}}(r) \end{vmatrix}$ and $\mathbf{Q} = \begin{vmatrix} \mathbf{Q_0} \\ \mathbf{0} \end{vmatrix}$ to column vectors of 19 size, which are denoted by $\mathbf{X}^r(r)$ and $\mathbf{Q}^r$ and written as follow:

$$\begin{aligned}\mathbf{X^r}(r) = \{&\rho^0_{11}(\mathbf{r}), \rho^0_{22}(\mathbf{r}), \rho^0_{33}(\mathbf{r}), \rho^0_{44}(\mathbf{r}), \rho^0_{55}(\mathbf{r}), \rho^0_{66}(\mathbf{r}), \rho^0_{12}(\mathbf{r}), \\ &\rho^0_{21}(\mathbf{r}), \rho^0_{77}(\mathbf{r}), \rho^0_{88}(\mathbf{r}), \rho^0_{99}(\mathbf{r}), \tilde{\rho}_{43}(\mathbf{r}), \tilde{\rho}_{14}(\mathbf{r}), \\ &\tilde{\rho}_{52}(\mathbf{r}), \tilde{\rho}_{98}(\mathbf{r}), \tilde{\rho}_{24}(\mathbf{r}), \tilde{\rho}_{87}(\mathbf{r}), \tilde{\rho}_{51}(\mathbf{r}), \tilde{\rho}_{65}(\mathbf{r})\}.\end{aligned} \tag{14}$$

and

$$\mathbf{Q^r} = \{1,1,1,1,1,1,0,0,1,1,1,0,0,0,0,0,0,0,0\}/9. \tag{15}$$

(to save place, those column vectors are written as rows). The B matrix is reduced to 19 × 19 matrix B^r with a numbering of elements. The system [Eq. (13)] becomes

$$[\mathbf{A^r} + \lambda(r)\mathbf{B^r} - r_d^2\nabla^2]\mathbf{X^r}(r) = \mathbf{Q^r}, \tag{16}$$

where $\mathbf{A^r}$ regroups $\mathbf{A_0}$, $\mathbf{A}_+$, and $\mathbf{A}_-$.

To solve Eq. (16), we divide the r space into three parts, $0 < r < r_a$, $r_a < r < r_1$, and $r_1 < r < \infty$, with the three values of $\lambda(r)$ $\lambda_\infty/2\beta$, $\lambda/2\beta$, and 0. We consider now the following notations:

$$\mathbf{C_1} = \mathbf{A^r} + \lambda_\infty\mathbf{B^r}, \quad \mathbf{X^r}(r) = \mathbf{X^r_1}(r), \quad \text{for} \quad 0 < r < r_a,$$

$$\mathbf{C_2} = \mathbf{A^r} + \lambda\mathbf{B^r}, \quad \mathbf{X^r}(r) = \mathbf{X^r_2}(r), \quad \text{for} \quad r_a < r < r_1,$$

$$\mathbf{C_3} = \mathbf{A^r}, \quad \mathbf{X^r}(r) = \mathbf{X^r_3}(r), \quad \text{for} \quad r_1 < r < \infty.$$

We then have to solve

$$[\mathbf{C_i} - r_d^2\nabla^2]\mathbf{X^r_i}(r) = \mathbf{Q^r}, \quad i = 1,2,3, \tag{17}$$

with the conditions which represent the continuity of the stream,

$$\mathbf{X^r_1}(r \leqslant r_a) = \mathbf{0},$$

$$\mathbf{X^r_1}(r = r_a) = \mathbf{X^r_2}(r = r_a),$$

$$\mathbf{X^r_2}(r = r_1) = \mathbf{X^r_3}(r = r_1),$$

$$\mathbf{X^r_3}(r \to \infty) = \mathbf{Q^r},$$

$$\left.\frac{d\mathbf{X^r_1}}{dr}\right|_{r=r_a} = \left.\frac{d\mathbf{X^r_2}}{dr}\right|_{r=r_a},$$

$$\left.\frac{d\mathbf{X^r_2}}{dr}\right|_{r=r_1} = \left.\frac{d\mathbf{X^r_3}}{dr}\right|_{r=r_1}. \tag{18}$$

TABLE II. The expressions of the functions $F(r)$ and $G(r)$ and their derivatives according to the triplet exciton motion dimensionality n.

n	dv	$F(r)$	$F\prime(r)$	$G(r)$	$G\prime(r)$	∇^2
1	dr	$ch(r)$	$sh(r)$	e^{-r}	$-e^{-r}$	$\frac{d^2}{dr^2}$
2	$2\pi rdr$	$I_0(r)$	$I_1(r)$	$-K_0(r)$	$-K_1(r)$	$\frac{d}{rdr} + \frac{d^2}{dr^2}$
3	$4\pi r^2dr$	$\frac{sh(r)}{r}$	$\frac{ch(r) - sh(r)}{r^2}$	$\frac{e^{-r}}{r}$	$-\left(\frac{1+r}{r^2}\right)e^{-r}$	$\frac{2d}{rdr} + \frac{d^2}{dr^2}$

We diagonalize the $\mathbf{C_i}$, which gives $\mathbf{P_i C_i P_i^{-1}}$ and C_i^j the 19 eigenvalues of $\mathbf{C_i}$.

Now, we set $\boldsymbol{\xi}_i(r)=\mathbf{P_i^{-1}X_i^r}(r)$ and $\boldsymbol{\xi}_{i,0}=\mathbf{P_i^{-1}Q^r}$, so we have to solve 3×19 equations of the form

$$[C_i^j - r_d^2\nabla^2]\xi_i^j(r) = \xi_{i,0}^j \quad (i=1,2,3;j=1-19), \tag{19}$$

where the index j indicates the diagonal matrix elements $(C^j=C_{jj})$ or vector components.

These equations can be solved by considering the equation of the type $f(r)-r_d^2\nabla^2 f(r)=0$ which has two general solutions $F(r)$ and $G(r)$ such that $dF/dr(r=0)=0$ and $G(r\to\infty)=0$. The expressions of $F(r)$ and $G(r)$ and their derivatives according to the dimensionality are given in Table II.

We, therefore, obtain for Eq. (19) the three types of solutions which are written in the following form:

$$\xi_1^j(r) = \xi_{1,0}^j/C_1^j + \Phi_1^j F(\sqrt{C_1^j}r/r_d),$$

$$\xi_2^j(r) = \xi_{2,0}^j/C_2^j + \Phi_2^j F(\sqrt{C_2^j}r/r_d) + \Gamma_2^j G(\sqrt{C_2^j}r/r_d),$$

$$\xi_3^j(r) = \xi_{3,0}^j/C_3^j + \Gamma_3^j G(\sqrt{C_3^j}r/r_d). \tag{20}$$

With those expressions of the column vector components, we find $\mathbf{X_i^r}(r)=\mathbf{P_i}\boldsymbol{\xi}_i(r)$ as a function of 4×19 constants Φ_1^j, Φ_2^j, Γ_2^j, and Γ_3^j which can be determined by the boundary conditions given by Eq. (18).

We set $\mathbf{P}^r=\mathrm{col}(P_S)$ in the 19-reduced space and $\mathbf{P}^{rT}=\mathbf{P}^{r+}$ the raw vector, with the same numbering of elements that $\mathbf{X^r}$(r) and $\mathbf{Q^r}$; so the observable (fluorescence) is proportional to

$$R_s = 2\beta\int_{sample}\mathrm{Tr}[P_S\rho(\mathbf{r},t)]dv = 2\beta\mathbf{P}^{rT}\left[\int_0^{r_a}\lambda_\infty\mathbf{B}^r\mathbf{X}^r(r)dv + \int_{r_a}^{r_1}\lambda\mathbf{B}^r\mathbf{X}^r(r)dv\right] = 2\beta\mathbf{P}^{rT}[\mathbf{X}_1+\mathbf{X}_2], \tag{21}$$

where $\mathbf{X}_1$ vector is deduced from Eq. (33) (Ref. 11):

$$\mathbf{X}_1=\int_0^{r_a}\lambda_\infty\mathbf{B}^r\mathbf{X}^r(r)dv = (\mathbf{Q}^r + n/uP_2\xi_2'(u))V_a, \tag{22}$$

where $u=r_a/r_d$ and $V_a=r_a,\pi r_a^2$, or $4\pi r_a^3/3$ according to the triplet exciton motion dimensionality n ($n=1$, 2, or 3), and the component X_2^j of $\mathbf{X}_2$ is deduced from Eq. (35) of the same reference,

TABLE III. Triplet exciton ZFS parameters and ZFS tensor principal axis of anthracene crystal.

D^* (cm^{-1})	E^* (cm^{-1})	Triplet exciton ZFS tensor principal axis	Ref. 31
−0.0058	0.0327	$\begin{array}{c} \\ x \\ y \\ z \end{array}\begin{pmatrix} a & b & c' \\ 0.8878 & 0 & 0.4602 \\ 0.4602 & 0 & -0.8878 \\ 0 & 1 & 0 \end{pmatrix}$	

$$\mathbf{X}_2^j = \int_{r_a}^{r_1}\lambda\mathbf{B}^r\mathbf{X}^r(r)dv = \lambda C_1^j\{(Q^r)^j/C_2^j(V_1-V_a) + n/C_2^j[V_1/u_1(\mathbf{P}_2\xi_2')(u_1))^j - V_a/u(\mathbf{P}_2\xi_2'(u))^j], \tag{23}$$

where $u_1=r_1/r_d$ and $V_1=r_1$, πr_1^2, or $4\pi r_1^3/3$.

The relative microwave effect on the delayed fluorescence signal $\Delta F/F$, ($\Delta F=F'-F$, F' and F being the signals under and without microwave perturbation) is finally obtained from Eq. (21),

$$\frac{\Delta F}{F} = \frac{R_s' - R_s}{R_s}. \tag{24}$$

III. APPLICATION TO FLUORESCENCE DETECTED MAGNETIC RESONANCE SPECTRUM OF A TWO-DIMENSIONAL CRYSTAL (ANTHRACENE)

The theory as given by Eqs. (21) and (24) in the high-field limit was numerically applied to FDMR spectrum of anthracene (see the Ref. 28 for experimental setup). This material is 2D motion system with an isotropic diffusion constant $D=D_{aa}=D_{bb}=1.5\times 10^{-4}$ cm^2 s^{-1} in the ab plane.[20,30]

Figure 1 shows the best fit (open circles) obtained from Eqs. (21) and (24) for the reported experimental FDMR spectrum (solid curve) for a static field lying in the ab diffusion plane parallel to the crystal a axis. The fit is obtained using the exciton ZFS parameters (Table III) and the microwave-radiation parameters $H_1=4$ Oe, $\omega/2\pi=9.4$ GHz, and as disposable parameters, the effective decay rate β and the long-range annihilation rate λ. The fit (open circles) is derived for $\beta=2.8\times 10^8$ s^{-1}, $\lambda=2.2\times 10^9$ s^{-1}, $r_a=5.23$ Å and $r_1=15.69$ Å. The used functions $F(r)$ and $G(r)$ and their derivatives are those given in Table II for $n=2$.

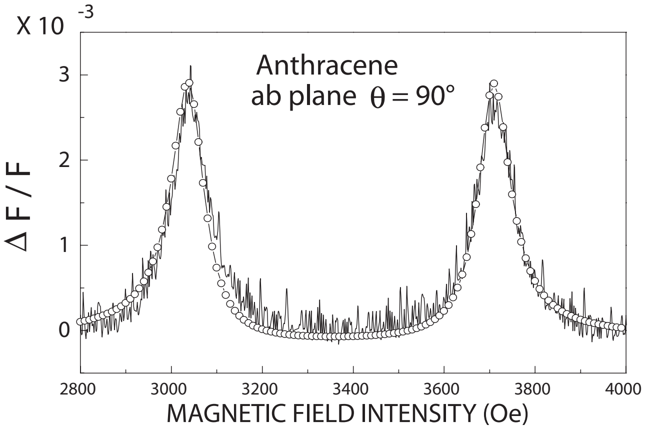

FIG. 1. Best fit of experimental FDMR spectrum for anthracene crystal. Solid curve is the FDMR experimental spectra at room temperature with the field lying in the ab plane and making a $\varphi=0°$ angle with the crystal a axis. Open circles correspond to the fit obtained with expressions (21) and (24).

TABLE IV. Used parameters for the best fit to experimental curve of DBN crystal.

Interactions	C_{1-m}	r_a (Å)	β (10^8 s^{-1})	λ (10^9 s^{-1})
Intrastack $(i-i)$	0.075	4.05	0.8	2
Intrastack $(i'-i')$	0.15	4.05	5	1
Interstack intrasite $(i-j,\, i'-j')$	0.075	14	3	1
Interstack intersite $(i-j')$	0.7	10	2.1	1

IV. APPLICATION TO FLUORESCENCE DETECTED MAGNETIC RESONANCE SPECTRUM OF A QUASI-ONE-DIMENSIONAL CRYSTAL (1,4 DIBROMONAPHTALENE)

1,4 DBN is considered to be a one-dimensional motion system,[32] with diffusion constant $D=D_{cc}=3.5 \times 10^{-4}$ cm^2 s^{-1} along the *c* axis.[21] The molecules are piled up as stacks along $\mathbf{c}'=\mathbf{a}\wedge\mathbf{b}$. Intrastack and interstack hoppings of excitons can occur. There are eight molecules per cell arranged into four units of two molecules each noted *i* and *j*′ ($i=1,\ldots,4$ and $j'=1,\ldots,4$) related by no symmetry elements (Fig. 1 of Ref. 28). Three types of triplet interactions can be considered,[33] intrastack $i-i$ or $i'-i'$ (e.g., $1-1$ or $1'-1'$, 8 interactions), interstack intrasite $i-j$ or $i'-j'$ (e.g., $1-2$ or $1'-2'$, 12 interactions), and interstack intersite $i-i'$ and $i-j'$ (e.g., $1-1'$ or $1-2'$, 16 interactions) [Table III (Ref. 23)].

Strictly speaking, we ought to find 36 values of $\lambda(r)$ if we consider only the interactions between excitons having a diffusion motion on the nearest stacks (whatever the site). Due to the symmetry relations in unit cell, the number of interactions is reduced; stacks related by inversion give identical results (e.g., $1-2$ is equivalent to $3-4$, it is the same for $1'-2'$ and $3'-4'$). Delayed fluorescence is then the sum of four contributions and its modulation by the microwave power can be expressed by[28]

$$\frac{\Delta F}{F} = C_{i-i}\left(\frac{\Delta F}{F}\right)_{i-i} + C_{i'-i'}\left(\frac{\Delta F}{F}\right)_{i'-i'} + C_{i-j}\left(\frac{\Delta F}{F}\right)_{i-j} + C_{i-j'}\left(\frac{\Delta F}{F}\right)_{i-j'}, \tag{25}$$

where C_{l-m} represents the normalized probability for each family of interactions (Table IV).

Figure 2 shows the best fit (open circles) obtained with expressions (21), (24), and (25) for the reported experimental FDMR spectrum at room temperature (solid curve) for the direction of the static magnetic field; $\theta=150° \pm 1°$, $\varphi=0°$ in the 1,4 DBN crystal.

The fit is obtained using the exciton ZFS parameters reported in Table II (Ref. 28), the action radius r_a (given in Table IV, for each interaction type) is deduced from the lattice spacing parameters and the relative position of molecules in *ab* plane (see Fig. 1 of Ref. 28), the interaction radius is $r_1=3r_a$, and the microwave-radiation parameters $H_1=2.2$ Oe and $\omega/2\pi=9.4$ GHz. The used parameters for the best fit to the experimental curve are regrouped in Table IV.

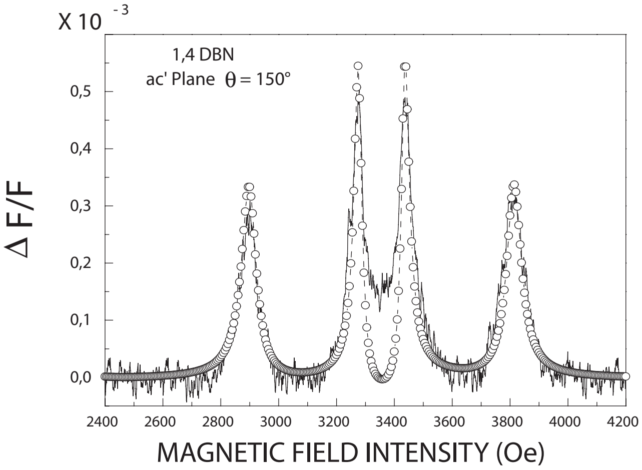

FIG. 2. Best fit of experimental FDMR spectra for 1,4 DBN crystal. Solid curve is the FDMR experimental spectra at room temperature with the field lying in the *ab* plane and making the angle $\theta=150°$ with the crystal *c* axis. Open circles correspond to the fit obtained with expressions (21), (24), and (25).

The FDMR resonances show that there is enough interstack interactions, in 1,4 DBN crystal, to allow annihilation to occur between triplets localized on different neighboring stacks. The difference between the intensities of FDMR lines indicates that this interaction is smaller than the intrastack triplet-triplet interaction.

V. DISCUSSION AND SUMMARY

The approach taken in this paper differs considerably from that of Johnson and Merrifield, who have presented a simplified model, which although rather crude has the advantage of lending itself to a simple physical interpretation and of providing a vivid qualitative understanding of the phenomenon. The work of Suna is more closely related to ours. It includes both the quantum-mechanical aspects of the recombination process and the spatial motion of triplet excitons on the lattice. The main differences are the proposed definition of the annihilation rate $\lambda(r)$ (to account for, the first, the second, or the third near-neighbor interactions of triplet excitons) and the use of superoperator formalism to solve the SLE. To keep the presentation and the calculation as simple as possible in order to emphasize the main points of the theory, we neglected the spin relaxation. If necessary, spin relaxation can be included in the model without any fundamental changes (by adding the Redfield supermatrix to Eq. (8) as in Ref. 11). The half widths at half maximum of the experimental resonance lines provide us the effective decay rates.[25] For anthracene crystal, the half widths at half maximum $\Delta H=(36\pm 3)$ Oe corresponding to $\beta=(2.3\pm 0.2) \times 10^8$ s^{-1}. For 1,4 DBN crystal, there is two values of ΔH: one for intrastack interaction ($\Delta H_{intrastack}$) and one for interstack interaction ($\Delta H_{interstack}$). The values are $\Delta H_{intrastack}=(30\pm 3)$ Oe and $\Delta H_{interstack}=(34\pm 3)$ Oe corresponding to $\beta_{intrastack}$ $(1{,}4\ \mathrm{DBN})=(1.6\pm 0.2)\times 10^8$ s^{-1} and

$\beta_{interstack}$ (1,4 DBN) = $(2.0\pm 0.2)\times 10^{8}$ s^{-1}. These values are in agreement with those provided by our treatment.

The experimental FDMR spectra of 2D and 1D triplet exciton motion systems, respectively, for anthracene and 1,4 DBN crystals are well reproduced using the parameters λ, β, r_a, and r_1, while one needs to introduce experimental half widths in calculus to obtain satisfactory fits for JM and Suna models.

---

[1] L. Altwegg and I. Zschokke-Granacher, Phys. Rev. B **20**, 4326 (1979).
[2] H. Bouchriha, V. Ern, J. L. Fave, C. Guthmann, and M. Schott, Phys. Rev. B **18**, 525 (1978).
[3] V. M. Kenkre, Phys. Rev. B **22**, 2089 (1980).
[4] P. Sibani and J. B. Pedersen, Phys. Rev. B **26**, 2584 (1982).
[5] V. Ern and A. Fort, Mol. Cryst. Liq. Cryst. **100**, 1 (1983).
[6] L. S. Swanson, J. Shinar, and K. Yoshino, Phys. Rev. Lett. **65**, 1140 (1990).
[7] L. S. Swanson, P. A. Lane, J. Shinar, and F. Wudl, Phys. Rev. B **44**, 10617 (1991).
[8] X. Wei, B. C. Hess, Z. V. Vardeny, and F. Wudl, Phys. Rev. Lett. **68**, 666 (1992).
[9] Q. X. Ni, L. S. Swanson, P. A. Lane, J. Shinar, Y. W. Ding, S. Ijadi-Maghsoodi, and T. J. Barton, Synth. Met. **49**, 447 (1992).
[10] L. S. Swanson, J. Shinar, Y. W. Ding, and T. J. Barton, Synth. Met. **1**, 55 (1993).
[11] A. Ben Fredj, S. Romdhane, J. L. Monge, and H. Bouchriha, J. Phys. I **7**, 349 (1997).
[12] V. Dyakonov, G. Rösler, M. Schwoerer, and E. L. Frankevich, Phys. Rev. B **56**, 3852 (1997).
[13] A. P. Monkman, H. D. Burrows, M. da G. Miguel, I. Hamblett, and S. Navaratnam, Chem. Phys. Lett. **307**, 303 (1999).
[14] Yu. V. Romanovskii, A. Gerhard, B. Schweitzer, U. Scherf, R. I. Personov, and H. Bässler, Phys. Rev. Lett. **84**, 1027 (2000).
[15] A. P. Monkman, H. D. Burrows, L. J. Hartwell, L. E. Horsburgh, I. Hamblett, and S. Navaratnam, Phys. Rev. Lett. **86**, 1358 (2001).
[16] M. Wohlgenannt, K. Tandon, S. Mazumdar, S. Ramasesha, and Z. V. Vardeny, Nature (London) **409**, 494 (2001).
[17] T. Barhoumi, S. Romdhane, A. Benfredj, F. Kouki, and H. Bouchriha, Synth. Met. **130**, 111 (2002).
[18] A. Benfredj, S. Romdhane, and H. Bouchriha, Synth. Met. **150**, 241 (2005).
[19] R. C. Johnson and R. E. Merrifield, Phys. Rev. B **1**, 896 (1970).
[20] A. Suna, Phys. Rev. B **1**, 1716 (1970).
[21] V. Ern, Chem. Phys. Lett. **56**, 6259 (1972).
[22] V. Ern, P. Avakian, and R. E. Merrifield, Phys. Rev. **148**, 862 (1966).
[23] A. Ben Fredj, D. Gamra, S. Romdhane, T. Barhoumi, C. Guthmann, J. L. Monge, and H. Bouchriha, Eur. Phys. J. B **19**, 385 (2001).
[24] M. Mejatty, J. L. Monge, V. Ern, and H. Bouchriha, Phys. Rev. B **36**, 2735 (1987).
[25] M. Mejatty, J. L. Monge, V. Ern, and H. Bouchriha, Phys. Rev. B **43**, 2558 (1991).
[26] E. L. Frankevich, V. Lesin, and A. I. Pristupa, Sov. Phys. JETP **48**, 208 (1978).
[27] J. L. Monge, M. Mejatty, V. Ern, and H. Bouchriha, J. Phys. (Paris) **47**, 659 (1986).
[28] A. Benfredj, F. Henia, L. Hachani, S. Romdhane, and H. Bouchriha, Phys. Rev. B **71**, 075205 (2005).
[29] K. A. McLauchlan and U. E. Steiner, Mol. Phys. **73**, 241 (1991).
[30] P. Avakian and A. Suna, Mater. Res. Bull. **6**, 891 (1971).
[31] D. Haarer and H. C. Wolf, Mol. Cryst. Liq. Cryst. **10**, 359 (1970).
[32] D. M. Moran, P. S. May, and F. S. Richardson, Chem. Phys. **186**, 77 (1994).
[33] H. Bouchriha, V. Ern, J. L. Fave, C. Guthmann, and M. Schott, Chem. Phys. Lett. **53**, 288 (1978).